Journal of Materials Chemistry C

Accepted Manuscript

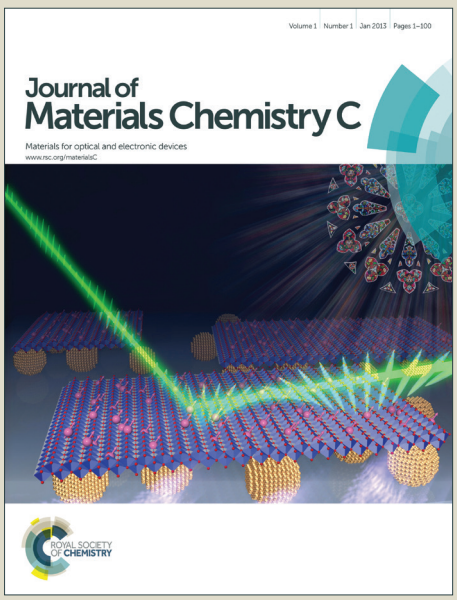

ROYAL SOCIETY OF CHEMISTRY

www.rsc.org/materialsC

ARTICLE TYPE www.rsc.org/xxxxxx | XXXXXXXX

Novel Series of Quaternary Fluoride Nanocrystals: Room-Temperature Synthesis and Down-Shifting/Up-Converting Multicolor Fluorescence

Xianghong He, Bing Yan*

Department of Chemistry, Tongji University, Siping Road 1239, Shanghai 200092, China

Received (in XXX, XXX) Xth XXXXXXXXX 200X, Accepted Xth XXXXXXXXX 200X
First published on the web Xth XXXXXXXXX 200X
DOI: 10.1039/b000000x

We have developed a straightforward wet-chemical approach for the preparation of pure-phase M_2NaScF_6 (M = K, Rb, Cs) quaternary fluoride nanocrystals at ambient conditions without high-temperature calcination or sophisticated experimental setups. The production of nanocrystals is highly dependent on the chelating agent, the feed ratio of chelating agent to Sc^{3+}, and the feed ratio of (KOH+NaOH) to Sc^{3+}. Down-shifting and up-converting multicolor fluorescence involving red, blue-white, green, and NIR can be realized by incorporating lanthanide dopants into these host lattices at room-temperature. Especially, single-band up-converting and down-shifting dual-modal emissions were achieved. The findings demonstrated that these hexafluoroscandates are versatile hosts for down-shifting and up-converting multicolor fluorescence. This solution-phase procedure is suitable for lab-scale and industrial production of nanocrystals without high-temperature annealing, and can be extended to the fabrication of other polynary rare earth fluorides.

Introduction

On account of the excellent optical/magnetic properties, exceptional stability, and high flexibility in choosing dopant and host matrix, lanthanide-doped rare-earth fluorides nanomaterials have a wide range of promising applications spanning from lighting, laser and display, over biological labeling, sensing, imaging, and photodynamic therapy, to silicon solar cells.[1] Therefore, over the last decades, extensive efforts have been dedicated to the development of synthetic strategies for obtaining rare-earth fluoride nanoparticles with controlled phase, morphology and chemical composition.[1h,2] Among these approaches, thermal decomposition of metal trifluoroacetate precursors,[2a-2d] high temperature coprecipitation,[2e–2h] and hydro/solvo-thermal technique,[1h,2i–2m] are nowadays the three most common routes.[1c,2a] Although good control over phase, morphology, and composition of fluoride nanocrystals (NCs) can be realized in these methods, the pyrolysis of metal trifluoroacetates produces very toxic fluorinated and oxyfluorinated carbon species, which always raises some safety concerns.[2a,2e–2h] In addition, these approaches still suffer from problems including complicated experimental conditions, tedious procedures, and high reaction temperatures (for example, usually exceeding 300 °C for the former, ≥ 280 °C for the latter, and ≥ 180 °C for the hydro/solvo-thermal).[1a,1d] In general, beyond obvious energetic concerns, a high temperature required for these routes is also a major barrier to the implementation of large-scale reproduction of NCs.[3] Hence, from safety and energy-saving standpoints, the development of a facile room-temperature (RT) solution-phase method to fabricate pure-phase fluoride-based NCs is still eagerly demanded.

On the other hand, in comparison with considerable work on binary and ternary rare-earth fluorides,[1b,2k] scandium-containing quaternary systems as phosphor matrix have largely been neglected. [4] Very recently, our group reported the fabrication and luminescence properties of a novel scandium-based quaternary fluoride host compound.[4a] Another scandium-containing quaternary fluoride systems M_2NaScF_6 (M = K, Rb, Cs) has been identified as model systems for investigating crystal-field and vibronic-coupling effects.[5] Moreover, they provide excellent platforms for the incorporation of a broad range of photo-active rare-earth ions since their elpasolite structure can accommodate trivalent ions in a site of rigorous octahedral symmetry without charge compensation.[5e-5j] Consequently, these scandium-based fluorides are expected to act as down-shifting (DS) and up-converting (UC) photoluminescent hosts for lanthanide activators. To the best of our knowledge, a synthesis procedure which allows the production of pure-phase M_2NaScF_6 (M = K, Rb, Cs) nanocrystallines at ambient conditions has not been reported up to now. Furthermore, it is still highly challenging to obtain single-band UC phosphors based on M_2NaScF_6 (M = K, Rb, Cs) matrices. In the present contribution, we successfully prepared M_2NaScF_6 (M = K, Rb, Cs) hexafluoroscandate NCs via a convenient RT solution-phase procedure. The functionalization of these NCs by means of doping strategy was demonstrated. Down-shifting and up-converting multicolor dual mode fluorescence has been realized in these scandium-based family matrices.

Experimental Section

Chemicals and Materials

All of the reagents and solvents were used as received without further purification. Analytical grade rare earths (RE) oxides (Sc_2O_3, Eu_2O_3, Tb_4O_7, Dy_2O_3, Sm_2O_3, Yb_2O_3, Er_2O_3, Tm_2O_3 and Ho_2O_3, 99.99%), $Ce(NO_3)_3{\cdot}6H_2O$ (≥ 99.95%), NaOH (≥ 96.0%), KOH (≥ 85.0%), HF (≥ 40.0%), concentrated nitric acid (HNO_3, ≥ 68.0%), ethanol (≥ 99.7%), citric acid monohydrate (≥ 99.8%), and cyclohexane (≥ 99.5%) were purchased from Sinopharm Chemical Reagent Co., China. RbOH (≥ 99.9%), $CsOH{\cdot}H_2O$ (≥ 99.9%), leinoleic acid (95 wt.%), and oleic acid (90 wt.%) were supplied by Alfa Aesar Co., China. Rare earths oxides were separately dissolved in dilute HNO_3 solution and the residual HNO_3 was removed by heating and evaporation, resulting in the formation of aqueous solution of corresponding $RE(NO_3)_3$.

Synthesis

All of the reagents and solvents were used as received without further purification. M_2NaScF_6 (M = K, Rb, Cs) hosts and lanthanide-doped M_2NaScF_6 NCs were prepared via a solution-phase method at room-temperature (25 ℃). Herein took the synthesis of K_2NaScF_6 NCs as an example. In a typical

preparation, NaOH (3.33 mmol, 0.14 g), KOH (6.67 mmol, 0.44 g), 6.0 mL deionized water, 10.0 mL alcohol, and 16.10 g oleic acid (or 16.0 g leinoleic acid, 1.27 g citric acid) were mixed together in a plastic beaker under stirring at room-temperature, followed by the addition of 4.00 mL aqueous solution of $Sc(NO_3)_3$ (0.25 M). The mixture was stirred vigorously for 2 hours. Subsequently, a stoichiometric amount of HF (0.31g) was slowly added into the mixture. After continually stirring for 30 min, the mixture was left to stand for 12 hours at 25 ℃. The products were collected by centrifugation, washed sequentially with cyclohexane, water and ethanol for several times. After dried in a vacuum at room-temperature for 24 hours, K_2NaScF_6 powder was obtained. Other Sc^{3+}-cintaining fluorides hosts were synthesized the same way, except that KOH was replaced with RbOH or CsOH. The above process can be extended to the preparation of lanthanide-doped M_2NaScF_6 (M = K, Rb, Cs) NCs, except that the stoichiometric amounts of $Sc(NO_3)_3$ and $RE(NO_3)_3$ (RE = Eu^{3+}, Ce^{3+}/Tb^{3+}, Dy^{3+}, Sm^{3+}, Yb^{3+}/Er^{3+}, Yb^{3+}/Ho^{3+}, Yb^{3+}/Tm^{3+}) mixed solutions were added into the initial mixture.

Characterization

The crystallographic structure and phase purity were determined by powder X-ray diffraction (XRD) using a Bruker D8 Advanced X-ray diffractometer with Ni filtered Cu K_α radiation (λ = 1.5406 Å) at a voltage of 40 kV and a current of 40 mA. The morphology and chemical composition of the samples were characterized on a Hitachi S4800 field-emission scanning electron microscope (SEM) equipped with an energy dispersive X-ray spectroscope (EDS). The photoluminescence properties were investigated in the solid state. Up-converting and down-shifting fluorescence spectra were collected on an Edinburgh Instruments FLS920 phosphorimeter using a 980 nm laser diode Module (K98D08M-30mW, China), and 450 W xenon lamp as excitation source, respectively. For low-temperature measurements (77 K), a Dewar equipped with optical glass windows was filled with liquid nitrogen (N_2). Raman backscattering measurements were performed using a Renishaw inVia spectrophotometer equipped with an Olympus microscope, a liquid-N_2-cooled CCD detector, and an Ar^+ ion laser (λ = 514.5 nm, 30 mW) as the exciting source.

Results and discussion

The Origin of This Work and Descriptive Synthetic Chemistry

The idea of this work was inspired by our initial attempts to prepare M_2NaScF_6 (M = K, Rb, Cs) nanocrystallines via a modified solvothermal method (the detailed procedure is given in ESI). Different treatment temperatures including 120, 150, 180, and 200 °C, were utilized to fabricate pure-phase nanocrystallines. As expected, the as-obtained products belonged to M_2NaScF_6 (M = K, Rb, Cs) nanoparticles shown in Figs. S1, S2, and S3 (ESI), which intrigues our further interest in the synthesis of M_2NaScF_6 (M = K, Rb, Cs) NCs under lower temperature. Even if the treatment temperature reached as lower as 50 °C, the as-synthesized samples unambiguously remained pure cubic NCs. Stimulated by this finding, we aimed to the ambient temperature synthesis of M_2NaScF_6 (M = K, Rb, Cs) hexafluoroscandates nanocrystallines. Pure-phase M_2NaScF_6 (M = K, Rb, Cs) nanoparticles were successfully fabricated by the RT reactions of NaOH, MOH (M = K, Rb, Cs), and $Sc(NO_3)_3$ with HF in a mixture of water, alcohol, and appropriate amount of chelating agent like oleic acid (OA). The overall synthetic procedure is depicted in Scheme 1.

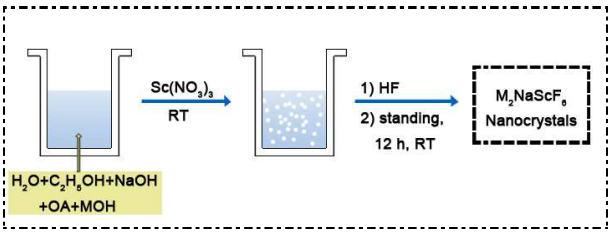

Scheme 1 Synthetic route to M_2NaScF_6 (M = K, Rb, Cs) NCs by a room-temperature (RT) solution-phase process.

As shown in Fig. 1a, X-ray diffraction (XRD) patterns of M_2NaScF_6 (M = K, Rb, Cs) samples exhibit sharp and intense peaks indicative of highly crystalline and can be well indexed as cubic K_2NaScF_6 (JCPDS no. 79-0770, space group Fm-3m), cubic Rb_2NaScF_6 (JCPDS no. 24-0970, space group Fm3m), and cubic Cs_2NaScF_6 (JCPDS no. 73-0341, space group Fm-3m), respectively. No trace of other characteristic peaks was observed for impurity phases. The calculated lattice constants are as follows: a = 8.482(1) Å for K_2NaScF_6, a = 8.593(2) Å for Rb_2NaScF_6, and a = 8.849(4) Å for Cs_2NaScF_6, which is in good agreement with the corresponding standard values for the bulk cubic M_2NaScF_6 (M = K, Rb, Cs). In the lattice structure of M_2NaScF_6 (M = K, Rb, Cs) compounds, the Sc^{3+} and Na^+ cations are octahedrally coordinated by six fluorine atoms. For each octahedron, the six Sc–F (or Na–F) bond lengths are equivalent. The M^+ cations are coordinated to 12 fluorine atoms, all of them at the same distance.[4c,5d,5e]

SEM images show that M_2NaScF_6 (M = K, Rb, Cs) samples are uniform quasi-spherical with a diameter ranging from 17 to 23 nm for K_2NaScF_6, 15 ~ 22 nm for Rb_2NaScF_6, and 46 ~ 90 nm for Cs_2NaScF_6 (Fig. 1b-1d). According to the Debye–Scherrer formula, the average crystallite sizes of M_2NaScF_6 (M = K, Rb, Cs) NCs were estimated as ~19, 17, and 85 nm, respectively, which matched well with the corresponding SEM results. Compositional analyses of the products using energy dispersive X-ray spectroscopy (EDS) (Fig. S4, ESI) confirm that the chemical signatures taken within different parts of the sample are identical within experimental accuracy and that the as-obtained samples contain Sc, Na, F, and K/Rb/Cs elements for K_2NaScF_6, Rb_2NaScF_6 and Cs_2NaScF_6, respectively. In addition, the actual atomic ratio of F, Sc, Na, and K/Rb/Cs elements were determined to be consistent with the designed nominal stoichiometry in each case. All above results confirmed that the M_2NaScF_6 (M = K, Rb, Cs) NCs can be successfully fabricated at RT through a facile solution-phase route.

It is well known that successful synthesis of single-phase NCs in a solution-based system not only depends on the intrinsic structure of the target compounds but also requires meticulous control of the experiment parameters such as feed ratio, reaction temperature, precursor, organic additives, and so forth.[3] In this work, to obtain phase pure M_2NaScF_6 (M = K, Rb, Cs) NCs, we carried out a set of experiments with synthetic parameters, including the chelating agent, the feed ratio of oleic acid to Sc^{3+}, and the feed ratio of (KOH+NaOH) to Sc^{3+}. K_2NaScF_6 was employed as an example compound to elucidate their roles in yielding high quality NCs. It is found that chelator, the feed molar ratio of oleic acid to Sc^{3+} as well as the feed molar ratio of (KOH+NaOH) to Sc^{3+} are three key factors responsible for the synthesis of single-phase NCs. Crystal phase analysis of products

under various synthetic parameters was summarized in Table S1 (ESI).

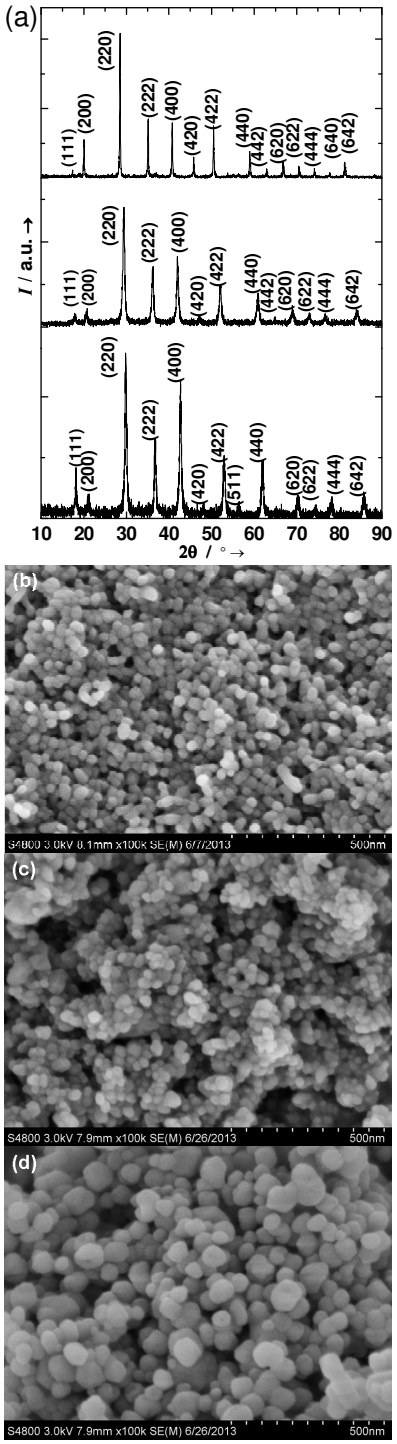

Fig. 1 a) XRD patterns of as-obtained K_2NaScF_6 (bottom curve), Rb_2NaScF_6 (middle curve), and Cs_2NaScF_6 (top curve) NCs (background uncorrected); SEM images of M_2NaScF_6 (M = K, Rb, Cs) NCs: b)K_2NaScF_6, c)Rb_2NaScF_6, d)Cs_2NaScF_6.

We firstly performed the synthesis of the samples under three different chelators such as OA, leinoleic acid, and citric acid. As the key assisting agent, the complexant was introduced into the reaction system to integrate all the metal ions including Na^+, K^+ (or Rb^+, Cs^+), and Sc^{3+} ions. For comparison, we also performed the synthesis of the sample without adding any chelator. XRD patterns of the samples without and with various chelating agents are shown in Fig. 2. In the absence of any chelator, K_2NaScF_6 as main phase was accompanied by ScOF, $NaOH{\cdot}4H_2O$, and NaOH impurity phases. When appropriate dose of OA (or leinoleic acid, citric acid) was added into the reaction system, single-phase K_2NaScF_6 NCs were generated. On the other hand, OA was selected as a representative to further reveal the effect of chelating agent on the generation of pure cubic NCs. The feed amount of OA varied under the same reaction condition to get a molar ratio of OA to Sc^{3+} of 1:1, 5:1, 10:1, 25:1, and 50:1. XRD patterns of the products are depicted in Fig. 3. When the OA to Sc^{3+} ratio kept 1:1, the reaction of NaOH, KOH, $Sc(NO_3)_3$, and HF yielded K_2NaScF_6 dominant phase as well as some impurity phases including ScOF, $NaOH{\cdot}4H_2O$, NaOH and NaF. Once the OA to Sc^{3+} ratio reached 5:1, single-phase K_2NaScF_6 nanoparticles was produced. With further increasing OA to Sc^{3+} ratio, the as-obtained products remained pure cubic NCs. Consequently, the presence of a certain amount of chelator is essential for the formation of phase-pure K_2NaScF_6. The chelating agents greatly helped to mediate the production of K_2NaScF_6 NCs through the interaction between carboxylic groups and metal ions, as an indispensable medium in the RT solution-phase reaction, which is similar to the role of ethylenediaminetetraacetic acid or OA for preparation of $NaYF_4$ based nanocrystalline and ultrasmall CeO_2 nanopartilces, respectively.[6]

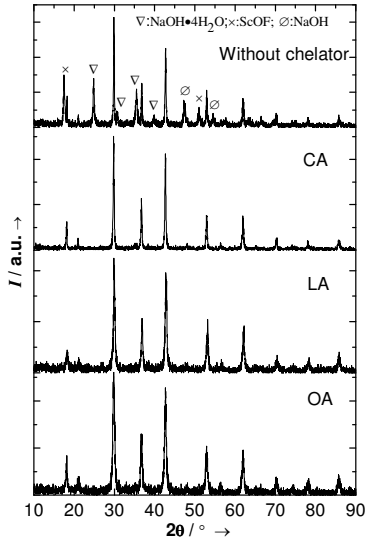

Fig. 2 XRD patterns of the products without and with various chelating agents (the molar ratio of chelating agent to Sc^{3+} remains 50:1): oleic acid (OA), leinoleic acid (LA), and citric acid (CA).

To investigate the role of KOH and NaOH, the total feed contents of (KOH+NaOH) including 3, 5, 10, 20, and 30 mmol were selected to examine the phase purity of products, while the feed amount of Sc^{3+} source and OA was fixed at 1 mmol and 50 mmol, respectively. Fig. 4 shows XRD patterns of the samples synthesized with different feed ratios of (KOH+NaOH) to Sc^{3+}. In the case of sample which is synthesized with (KOH+NaOH) content of 3 mmol (stoichiometric amount), a combination of cubic phase K_2NaScF_6 and some impurity phases including ScF_3, $KScF_4$, KSc_2F_7, $NaOH{\cdot}4H_2O$ and NaF was produced. When

excess amount of (KOH+NaOH) (5 mmol) [i.e. the ratio of (KOH+NaOH) to Sc^{3+} reached 5:1] was added in the system while other parameters were kept constant, pure-phase K_2NaScF_6 nanoparticles was obtained. Upon further increasing the content of (KOH+NaOH) to 20 and 30 mmol, pure cubic phase Sc^{3+}-containting compound was still obtained. The findings indicated that KOH and NaOH play an important role in the formation of K_2NaScF_6 pure-phase. Apart from acting as K^+ and Na^+ sources for K_2NaScF_6 NCs, KOH and NaOH also provided adequate OH^- ions for the precipitation of Sc^{3+}.[7]

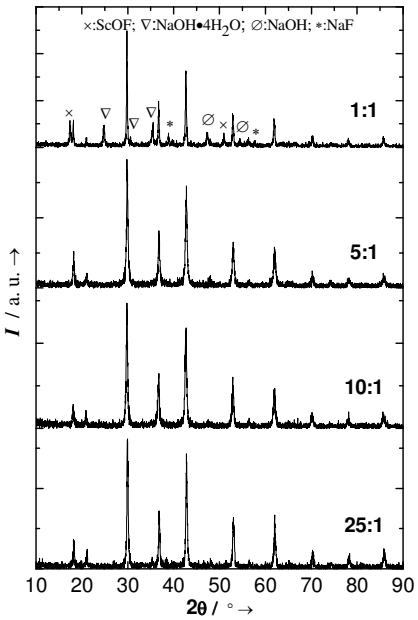

Fig. 3 XRD patterns of the as-obtained samples in the presence of different OA/Sc^{3+} feed ratio (1:1 ~ 25:1).

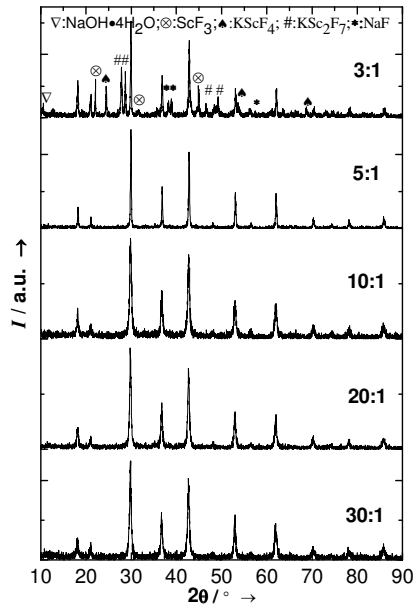

Fig. 4 XRD patterns of the samples derived at different feed ratio of (KOH+NaOH) to Sc^{3+} (3:1 ~ 30:1) in the presence of the fixed amounts of OA and Sc^{3+} sources.

DS and UC Fluorescence of Lanthanide-doped M_2NaScF_6 (M = K, Rb, Cs)

In aim to examine the feasibility of the as-obtained M_2NaScF_6 (M = K, Rb, Cs) as efficient and versatile host materials, doping with various photo-active lanthanide ions was conducted under experimental conditions identical with those employed for host samples. Fig.s 5(a) and S5 (ESI) depicted the RT DS excitation and emission spectra of M_2NaScF_6:Ln^{3+} [M = K, Rb, Cs; Ln = Eu (5 mol %), Dy (3 mol %), Ce/Tb (5/1 mol %), Sm (3 mol %)] nanophosphors. Under ultraviolet (UV) irradiation, these hexafluoroscandates based nanoparticles show multicolor visible emissions including red, blue-white, and green for Eu^{3+}- or Sm^{3+}-doped samples, Dy^{3+}-activated, and Ce^{3+}/Tb^{3+}-codoped NCs, respectively. The Commission Internationale de L'Eclairage (CIE) chromaticity coordinates for the emission spectra are calculated (Table S2, and Fig. S6, ESI).

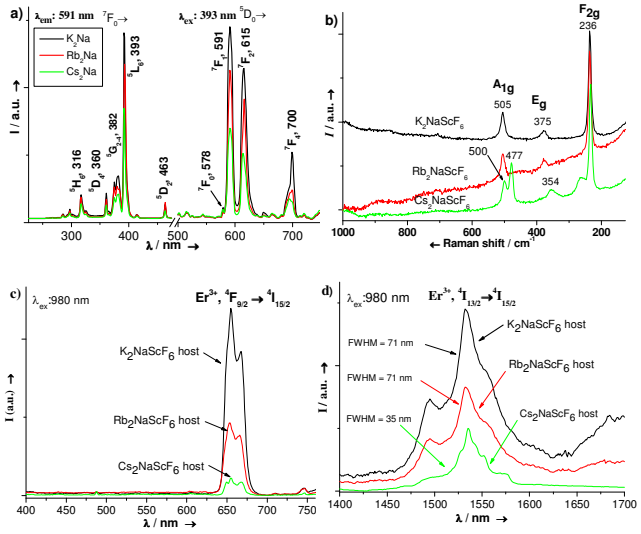

Fig. 5 a) DS photoluminescence excitation (left) and emission (right) spectra of M_2NaScF_6:Eu^{3+} (5 mol %) nanophosphors at RT, b) Raman spectra of M_2NaScF_6 hosts (the peak locations and their symmetry assignments are given), UC (c) and DS (d) emission spectra of M_2NaScF_6:Yb^{3+}/Er^{3+} (10/1 mol %) nanophosphors at RT (M = K, Rb, Cs).

Eu^{3+} is not only one of well-known activators for red-emitting phosphors, but also an excellent spectral probe to investigate the local crystal field in host lattices.[8] Hence, we chose Eu^{3+}-doped M_2NaScF_6 (M = K, Rb, Cs) NCs as an example to reveal whether these lanthanide ions have been successfully doped into host lattice. As shown in the left panel of Fig. 5(a), the excitation spectra of Eu^{3+}-activated Sc^{3+}-based NCs were dominated by the $^7F_0 \rightarrow {}^5L_6$ transition of Eu^{3+} ions centered at ~393 nm, and no obvious Eu^{3+}–O^{2-} charge transfer band (around 250-300 nm) was observed, indicating that all the as-prepared Sc^{3+}-containing NCs are free of oxygen (O^{2-} or OH^-).[8a,8b] These Eu^{3+}-activated samples exhibit an intense, characteristic luminescence of Eu^{3+} ions upon excitation with a radiation of 393 nm, in which the transitions from excited $^5D_0$ state to the different J levels (J = 0 - 4) of the lower ^7F state were observed, including $^5D_0 \rightarrow {}^7F_0$ at 578 nm, $^5D_0$ - $^7F_1$ at 591 nm, $^5D_0 \rightarrow {}^7F_2$ at 615 nm, $^5D_0 \rightarrow {}^7F_3$ at 650 nm, and $^5D_0 \rightarrow {}^7F_4$ at 700 nm.[8c] The presence of a single $^5D_0 \rightarrow {}^7F_0$ peak, in both the RT and 77 K luminescence (Fig. S7, ESI) spectra of the K_2NaScF_6:Eu^{3+}, implies that Eu^{3+} ion occupies a single site in host lattices.[8d–8g] The emission intensity of the $^5D_0$

$\rightarrow {}^7F_1$ (magnetic-dipole) is obviously stronger than that of the ${}^5D_0 \rightarrow {}^7F_2$ (electric-dipole) transition. According to the Judd–Ofelt theory, the intensity ratio of electric-dipole transition to magnetic-dipole transition, also called the asymmetric ratio, can be used to assess the symmetry of local crystal field in the vicinity of Eu^{3+} ions.[8d–8g] Lower asymmetric ratio typically indicates higher crystal field symmetry. Herein, the asymmetric ratio for Eu^{3+}-activated K^+-containing, Rb^+-containing, and Cs^+-containing NCs was calculated to be 0.88, 0.86, 0.83, respectively. As such, the lower asymmetric ratio evidences the incorporation of Eu^{3+} into a more symmetric environment.[8d–8g] All together, the above results suggest that Eu^{3+} ions have been successfully introduced into host lattices and are occupied a high symmetry site, i.e. Sc^{3+} sites with octahedral symmetry in M_2NaScF_6 (M = K, Rb, Cs) matrixes.[4c,5d,5e]

For Dy^{3+}, Ce^{3+}/Tb^{3+}, or Sm^{3+} doped NCs, as demonstrated in Fig. S5, the positions of excitation or emission peaks did not obviously shift. All the resulting nanophosphors show corresponding characteristic luminescence from dopants, indicating that Dy^{3+}, Ce^{3+}/Tb^{3+}, or Sm^{3+} ions were also successfully incorporated into M_2NaScF_6 (M = K, Rb, Cs) host lattices via the above approach at ambient conditions.

Raman spectra of M_2NaScF_6 (M = K, Rb, Cs) samples are shown in Fig. 5(b). The well-resolved sharp peaks indicated that all the samples were highly crystallized, which is in agreement with above XRD results. The strongest phonon mode is about 236 cm^{-1}, which is considerably lower than that of the widely studied rare-earth fluoride host lattices, such as $NaYF_4$ (~360 cm^{-1}),[8h,8i] and $LiYF_4$ (570 cm^{-1}).[9] It is well known that ideal host materials for efficient UC luminescence should have low lattice phonon energies, because lower phonon energies are an important aspect for minimizing nonradiative (multiphonon) losses as well as increasing the overall metastable energy lifetime of the UC processes.[1a] Obviously, the as-prepared M_2NaScF_6 (M = K, Rb, Cs) can be appointed as promising host lattices for efficient upconverter. To ascertain this point, Yb^{3+}/R^{3+} ion-pairs (R = Er, Tm, Ho) were added to form M_2NaScF_6:Yb^{3+}/R^{3+} (10/1 mol%, M = K, Rb, Cs) NCs. Upon excitation with a 980 nm laser diode, M_2NaScF_6:Yb^{3+}/Er^{3+} (10/1 mol%, M = K, Rb, Cs) NCs displays single-band deep-red luminescence, while the green (Fig. 5(c)), and near-infrared (NIR) luminescence can be observed in Yb^{3+}/Ho^{3+}, and Yb^{3+}/Tm^{3+} activated M_2NaScF_6 (M = K, Rb, Cs) (Fig. S8, ESI), respectively.

Fig. 5(c) depicts the RT UC emission spectrum of Yb^{3+}/Er^{3+} co-activated M_2NaScF_6 (M = K, Rb, Cs) NCs. In comparison with Yb^{3+}/Er^{3+} co-doped routine rare-earth-based fluorides NCs which typically exhibit multiple-band emissions in the visible spectral region,[1d,1e,1l,2a,4a,9] a nearly single-band red emission at around 655 nm for M_2NaScF_6:Yb^{3+}/Er^{3+} (M = K, Rb, Cs) was observed, while the green emission was almost entirely restrained. A similar phenomenon was also observed in $NaYF_4$:Yb^{3+}/Er^{3+} (10/1 mol %) NCs,[10] in which doping of Yb^{3+}/Er^{3+} ion-pair is in the same level as that of M_2NaScF_6:Yb^{3+}/Er^{3+} sample. Likewise, at the low-temperature (77 K) Yb^{3+}/Er^{3+}-codoped K_2NaScF_6 NCs remained a single-band UC emission (Fig. S9, ESI), indicating that the phonon participation in the transfer process has only a slight effect on the emission. We speculated that the almost banned green emission is related to the larger population of ${}^4F_{9/2}$ level of Er^{3+} ions in the presence of organic groups on the surfaces of NCs (See IR spectrum in Fig. S10, ESI).[10,11] The possible UC emission mechanism and simplified energy level diagram of Yb^{3+}/Er^{3+} are presented in Fig. S11 (ESI). In addition, the full width at half maximum (FWHM) of the red-emitting band is measured to be 26 nm, which is comparable to that (20 nm) for $KMnF_3$:Yb^{3+}/Er^{3+} NCs, but is narrower than the red-emitting band (~ 42 nm) of ZrO_2:Yb^{3+}/Er^{3+} NCs or the red-emitting band (~75 nm) for Y_2O_3:Yb^{3+}/Er^{3+} NCs.[12] It is obvious that both the most efficient excitation (980 nm) and emission peaks of as-obtained M_2NaScF_6:Yb^{3+}/Er^{3+} (10/1 mol %, M = K, Rb, Cs) are within the "optical window" of tissues, which can provide both deeper penetration of photons from the excitation and greater escape depths for the emission in biological samples, indicating that these nanophosphors are attractive for bio-labeling applications after appropriate surface modification.[1d,1e]

Er^{3+} is also one of the well-known efficient active centers for luminescent materials used in light amplifiers and optical fiber communication systems, because its emission at around 1.5 μm locates in the right position for the third telecommunication window.[13] Fig. 5(d) shows the NIR luminescence spectra of Er^{3+}-activated NCs excited by a 980 nm laser diode, a noticeable emission peak centered at ~1532 nm is detected, which is assigned to the typical ${}^4I_{13/2} \rightarrow {}^4I_{15/2}$ transition of Er^{3+} ions. To enable a wide-gain bandwidth for optical amplification, a broad emission band is always desirable.[13e,13f] Both K^+-containing and Rb^+-containing nanophosphors have appreciable FWHM value (71 nm), which enable a wide-gain bandwidth for optical amplification. These values are comparable to those observed for other Er^{3+} doped into inorganic hosts like LaF_3 (70 nm).[13a] The latter is a very good host in which Er^{3+} ions emits intense NIR luminescence in the telecommunication window.[13a]

Based on above findings, we can see that both the UC and DS multicolor fluorescence of red, blue-white, green, and even NIR can be realized in these host lattices by introducing appropriate lanthanide ions including Eu^{3+}, Dy^{3+}, and Sm^{3+} as activators, as well as Ce^{3+}/Tb^{3+}, Yb^{3+}/Er^{3+}, Yb^{3+}/Tm^{3+}, and Yb^{3+}/Ho^{3+} as sensitizer–activator pairs. Especially, Yb^{3+}/Er^{3+} co-doped nanophosphors exhibited dual mode luminescence involving single-band visible UC with narrow FWHM, as well as NIR DS with relatively large bandwidth upon excitation of 980 nm.

Conclusions

In summary, we have demonstrated for the first time the preparation of single-phase Sc^{3+}-containing quaternary fluorides NCs using a simple solution-phase method at ambient conditions. Incorporating of these hexafluoroscandates with photo-active lanthanide ions or ion-pairs illustrated their suitability as versatile hosts for down-shifting and up-converting multicolor fluorescence to develop nanomaterials with interesting applications in display devices, biological imaging, optoelectronics and telecommunications. The developed approach is suitable for large-scale production without the use of either high-temperature annealing or sophisticated experimental setups, as well as with high synthetic reproducibility. Our work opens up new perspectives for the development of polynary fluoride nanocrystals preparation at ambient temperature.

Acknowledgement

This work is supported by the National Natural Science Foundation of China (91122003) and Developing Science Funds of Tongji University.

Notes and references

[a] *Department of Chemistry, Tongji University, Shanghai, 200092, China. E-mail: byan@tongji.edu.cn; Fax: +86-21-65982287; Tel: +86-21-65984663*

† Electronic Supplementary Information (ESI) available: The solvothermal procedure of M_2NaScF_6 (M = K, Rb, Cs) nanocrystallines, XRD patterns, EDX analysis, crystal phase analysis, DS photoluminescence excitation and emission spectra, CIE chromaticity coordinates and diagrams, DS emission spectrum at 77 K, UC emission spectra, UC emission spectrum at 77 K, IR spectrum and schematic energy level diagram. See DOI: 10.1039/b000000x/

[1] (a) F. Wang, and X. Liu, *Chem. Soc. Rev.* **2009**, *38*, 976; (b) M. Haase, and H. Schäfer, *Angew. Chem. Int. Ed.* **2011**, *50*, 5808; (c) J. Chen and J. X. Zhao, *Sensors* **2012**, *12*, 2414;(d) D. Tu, Y. Liu, H. Zhu and X. Chen, *Chem. Eur J.* **2013**, *19*, 5516; (e) H. H. Gorris, and O. S. Wolfbeis, *Angew. Chem. Int. Ed.* **2013**, *52*, 3584;(f) X. Huang, S. Han, W. Huang, and X. Liu, *Chem. Soc. Rev.* **2013**, *42*, 173; (g) R. Naccache, F. Vetrone, and J. A. Capobianco, *ChemSusChem* **2013**, *6*, 1308; (h) F. Wang, Y. Han, C. S. Lim, Y. Lu, J. Wang, J. Xu, H. Chen, C. Zhang, M. Hong and X. Liu, *Nature* **2010**, *463*, 1061; (i) Q. Liu, Yun Sun, T. Yang, W. Feng, C. Li, and F. Li, *J. Am. Chem. Soc.* **2011**, **133**, 17122; (j) E. N. M Cheung, R. D. A Alvares, W. Oakden, R. Chaudhary, M. L Hill, J. Pichaandi, G. C. H Mo, C. Yip, P. M Macdonald, and G. J. Stanisz, *Chem. Mater.* **2010**, *22*, 4728; (k) J. Zhou, N. Shirahata, H. T. Sun, B. Ghosh, M. Ogawara, Y. Teng, S. Zhou, R. G. S. Chu, M. Fujii, and J. Qiu, *J. Phys. Chem. Lett.* **2013**, *4*, 402; (l) L. Liang, Y. Liu, C. Bu, K. Guo, W. Sun, N. Huang, T. Peng, B. Sebo, M. Pan, W. Liu, S. Guo, and X. Z. Zhao, *Adv. Mater.* **2013**, *25*, 2174; (m) Z. Gu, L. Yan, G. Tian, S. Li, Z. Chai, and Y. Zhao, *Adv. Mater.* **2013**, *25*, 3758.

[2] (a) J. C. Boyer, F. Vetrone, L. A. Cuccia, and J. A. Capobianco, *J. Am. Chem. Soc.* **2006**, *128*, 7444; (b) H. X. Mai, Y. W. Zhang, R. Si, Z. G. Yan, L. D. Sun, L. P. You, and C. H. Yan, *J. Am. Chem. Soc.* **2006**, *128*, 6426; (c) G. S. Yi, and G. M. Chow, *Adv. Funct. Mater.* **2006**, *16*, 2324; (d) X. Ye, J. E. Collins, Y. Kang, J. Chen, D. T. N. Chen, A. G. Yodh, and C. B. Murray, *Proc. Natl. Acad. Sci. USA 2010*, *107*, 22430; (e) Z. Q. Li, and Y. Zhang, *Nanotechnology* **2008**, *19*, 345606; (f) Z. Q. Li, Y. Zhang, and S. Jiang, *Adv. Mater.* **2008**, *20*, 4765; (g) H. T. Wong, F. Vetrone, R. Naccache, H. L. W. Chan, J. H. Hao, and J. A. Capobianco, *J. Mater. Chem.* **2011**, *21*, 16589; (h) X. Teng, Y. Zhu, W. Wei, S. Wang, J. Huang, R. Naccache, W. Hu, A. I. Y. Tok, Y. Han, Q. Zhang, Q. Fan, W. Huang, J. A. Capobianco and L. Huang, *J. Am. Chem. Soc.* **2012**, *134*, 8340; (i) X. Wang, J. Zhuang, Q. Peng, and Y. Li, *Nature*, **2005**, *437*, 121; (j) F. Zhang, Y. Wan, T. Yu, F. Zhang, Y. Shi, S. Xie, Y. Li, L. Xu, B. Tu, and D. Zhao, *Angew. Chem. Int. Ed.* **2007**, *46*, 7976; (k) C. X. Li, and J. Lin, *J. Mater. Chem.* **2010**, *20*, 6831; (l) Q. Zhang, and B. Yan, *Chem. Commun.* **2011**, *47*, 5867; (m) D. Chen, Y. Yu, F. Huang, and Y. Wang, *Chem. Commun.* **2011**, *47*, 2 601.

[3] D. V. Talapin, J. S. Lee, M. V. Kovalenko, and E. V. Shevchenko, *Chem. Rev.* **2010**, *110*, 389.

[4] (a) X. H. He, and B. Yan, *J. Mater. Chem. C* **2013**, *1*, 3910; (b) L. J. Andrews, S. M. Hitelman, M. Kokta, and D. Gabbe, *J. Chem. Phys.* **1986**, *84*, 5229; (c) C. Reber, H. U. Guedel, G. Meyer, T. Schleid, and C. A. Daul, *Inorg. Chem.***1989**, *28*, 3249; (d) C. Reinhard, K. Krämer, D. A. Biner, and H. U. Güdel, *J. Alloys Compd* **2004**, *374*, 133; (e) L. P. Sosman, R. J. M. Fonseca, A. D. Tavares, Jr., M. K. K. Nakaema, and H. N. Bordallo, *J. Fluore.* **2006**, *16*, 317; (f) B. Z. Malkin, D. S. Pytalev, M. N. Popova, E. I. Baibekov, M. L. Falin, K. I. Gerasimov, and N. M. Khaidukov, *Phys. Rev. B* **2012**, *86*, 134110.

[5] (a) M. G. Brik, and K. Ogasawara, *Phys. Rev. B* **2006**, *74*, 045105; (b) A. Trueba, P. Garcia-Fernandez, J. M. García-Lastra, J. A. Aramburu, M. T. Barriuso, and M. Moreno, *J. Phys. Chem. A* **2011**, *115*, 1423; (c) R. H. Bartram, G. R. Wein, and D. S. Hamilton, *J. Phys.: Condens. Matter* **2001**, *13*, 2377; (d) A. C. Doriguetto, T. M. Boschi, P. S. Pizani, Y. P. Mascarenhas, and J. Ellena, *J. Chem. Phys.* **2004**, *121*, 3184; (e) R. H. Bartram, G. R. Wein, and D. S. Hamilton, *J. Phys.: Condens. Matter* **2001**, *13*, 2363; (f) P. A. Tanner, C. S. K. Mak, W. M. Kwork, D. L. Phillips, and M. D. Faucher, *Phys. Rev. B-Cond. Matter Mater. Phys.* **2002**, *66*,1652031; (g) P. J. Dereń, W. Strek, E. Zych, and J. Drozdzyński, *Chem. Phys. Lett.* **2000**, *332*, 308; (h) M. A. Buñuel, L. Lozano, J. P. Chaminade, B.Moine, and B. Jacquier, *Opt. Mater.* **1999**, *13*, 211; (i) M. Campbell, W. Humbs, J. Strasser, H. Yersin, and C. D. Flint, *Proc. SPIE* **1997**, *3176*,103; (j) M. F. Joubert, S. Guy, S. Cuerq, and P. A. Tanner, *J. Lumine.* **1997**, *75*, 287.

[6] (a) G. Yi, H. Lu, S. Zhao, Y. Ge, W. Yang, D. Chen, and L. H. Guo, *Nano Lett.* **2004**, *4*, 2191; (b) T. S. Sreeremya, K. M. Thulasi, A.a Krishnan, and S. Ghosh, *Ind. Eng. Chem. Res.* **2012**, *51*, 318.

[7] L. Y. Bao, Z. Q. Li, Q. L. Tao, J. J. Xie, Y. Y. Mei, and Y. J. Xiong, *Nanotechnology* **2013**, *24*,145604.

[8] (a) F. Wang, Y. Zhang, X. P. Fan, and M. Q. Wang, *Nanotechnology* **2006**, *17*, 1527; (b) P. Ptacek, H. Schäfer, K. Kömpe, and M. Haase, *Adv. Func. Mater.* **2007**, *17*, 3843; (c) M. Shang, D. Geng, X. Kang, D. Yang, Y. Zhang, and J. Lin, *Inorg. Chem.* **2012**, *51*, 11106; (d) A. F. Kirby, and F. S Richardson, *J. Phys. Chem.* **1983**, *87*, 2557; (e) Stouwdam, J. W.; van Veggel, and F. C. J. M. *Nano Lett.* **2002**, *2*, 733; (f) C. Li, Z. Quan, J. Yang, P. Yang, and J. Lin, *Inorg. Chem.* **2007**, *46*, 6329; (g) A. C. A. Jayasundera, A. A. Finch, P. Wormald, and P. Lightfoot, *Chem. Mater.* **2008**, *20,* 6810; (h) J. F. Suyver, J. Grimm, M. K. van Veen, D. Biner, K. W. Krämer, and H. U. Güdel, *J. Lumin.* **2006**, *117*, 1; (i) S. A. Miller, H. E. Rast, and H. H. Caspers, *J. Chem. Phys.* **1970**, *52*, 4172.

[9] D. Q. Chen, L. Lei, J. Xu, A. P. Yang, and Y. S. Wang, *Nanotechnology* **2013**, *24*, 085708.

[10] J. Zhao, Y. Sun, X. Kong, L. Tian, Y. Wang, L. Tu, J. Zhao, and H. Zhang, *J. Phys. Chem. B* **2008**, *112*, 15666.

[11] (a) J. H. Zeng, T. Xie, Z. H. Li, and Y. Li, *Cryst. Growth Des.* **2007**,7, 2774; (b) Y. Liu, Q. Yang, and C. Xu, *J. Appl. Phys.* **2008**, *104*, 064701-064701-5; (c) Y. Liu, Q. Yang, G. Ren, C. Xu, and Y. Zhang, *J. Alloys Compd* **2009**, *467*, 351; (d) G. Tian, Z. Gu, X. Liu, L. Zhou, W. Yin, L. Yan, S. Jin, W. Ren, G. Xing, S. Li, and Y. Zhao, *J. Phys. Chem. C* **2011**, *115*, 23790.

[12] (a) J. Wang, F. Wang, C. Wang, Z. Liu, and X. G. Liu, *Angew. Chem. Int. Ed.* **2011**, *50*, 10369; (b) G. Y. Chen, Y. G. Zhang, G. Somestalean, Z. G. Zhang, Q. Sun, and F. P. Wang, *Appl. Phys. Lett.* **2006**, *89*, 163105; (c) D. Matsuura, *Appl. Phys. Lett.* **2002**, *81*, 4526.

[13] (a) J. W. Stouwdam, and F. C. J. M. van Veggel, *Nano Lett.* **2002**, *2*, 733; (b) J. C. G. Bünzli, and S. V. Eliseeva, *J. Rare Earths* **2010**, *28*, 824; (c) X. Zhai, S. Liu, X. Liu, F. Wang, D. Zhang, G. Qin, and W. Qin, *J. Mater. Chem. C* **2013**, *1*, 1525; (d) A. Mech, A. Monguzzi, F. Meinardi, J. Mezyk, G. Macchi, and R. Tubino, *J. Am. Chem. Soc.* **2010**, *132*, 4574; (e) O. H. Park, S. Y. Seo, B. S. Bae, and J. H. Shin, Appl. Phys. Lett. **2003**, *82*, 2787; (f) J. S. Kumar, K. Pavani, M. P. F. Graça, M. J. Soares, and M. A. Valente, *Phys. Status Solidi B* **2013**, *250*,837.